Ion beams and lasers

New directions for surface analysis.

Barbara J. Garrison
Nicholas Winograd

Shooting atom-sized bullets into unsuspecting crystals and analyzing the way these particles alter their targets can give surface scientists valuable information about the chemistry and structure of those solids. In a 1987 CHEMTECH article, Michael Kelley noted that these ion beam methods are experiencing a renaissance when used to characterize surfaces (*1*). Ion beams can provide high sensitivity, lateral resolution of <1 micron, and quantitative molecular analysis of polymer surfaces. Moreover, these features can be achieved by using less than one bombarding atom per thousand surface atoms, limiting surface damage.

Although Kelley concluded that the ion beam is a powerful tool that has attracted less attention than it deserves, that situation is slowly changing. In this article, we will demonstrate how coupling lasers with ion beams opens up a whole horizon of new applications. These applications involve molecular surface analysis with unprecedented sensitivity, as well as the possibility of performing detailed chemical analysis with submicron spatial resolution. The ion beam method of interest here goes by the various names of sputtering, secondary ion mass spectrometry (SIMS), and fast atom bombardment mass spectrometry (FABMS). We will not discuss the techniques of ion scattering spectrometry (ISS) and Rutherford back scattering spectroscopy (RBS), which were also covered by Kelley.

In SIMS (and FABMS and sputtering) a particle with 1–25 keV of kinetic energy strikes a solid surface. As the attractive forces that hold the solid together are only 3–6 eV, considerable motion is induced in the solid (Figure 1). Eventually a few particles escape from the solid and can be detected. There is tremendous damage in the

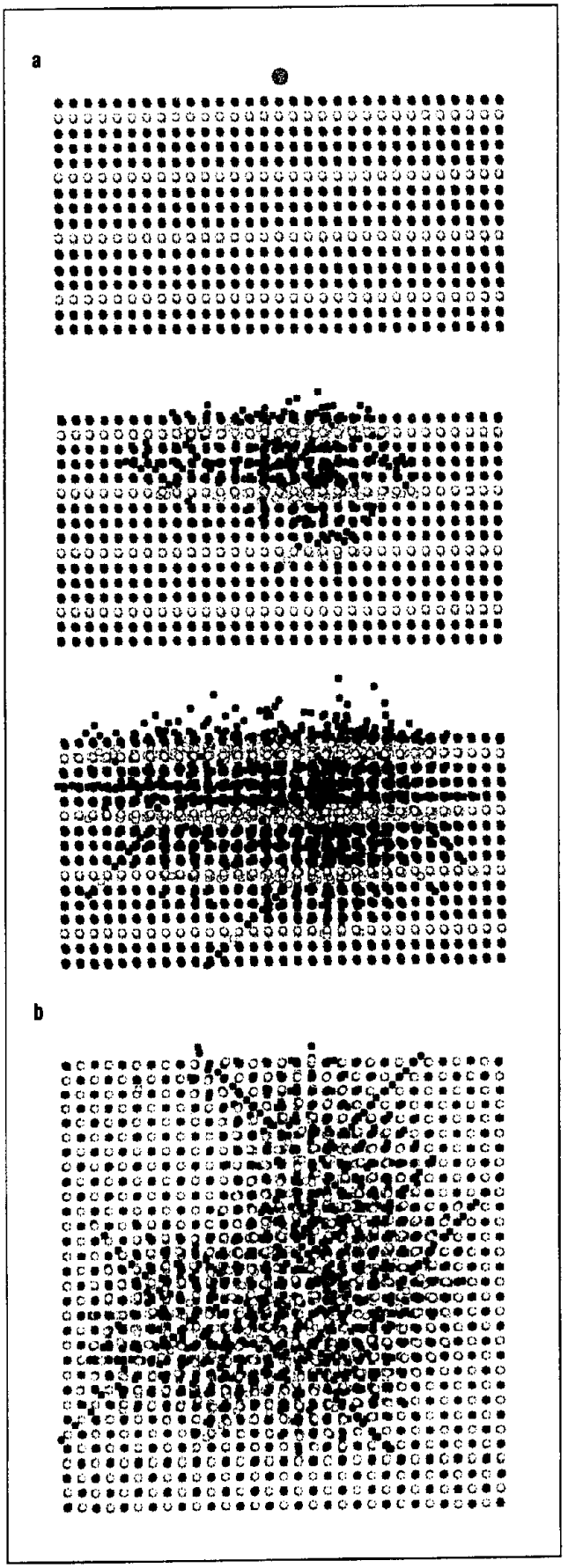

Figure 1. **Time snapshots from a molecular dynamics simulation for 3 keV Ar^+ ion bombardment of Rh metal. The atoms are colored by layer.** (a) Side view, from top to bottom, at times 0, 100 fs, and 200 fs; (b) Top view at 200 fs.

0009–2703/93 $4.00

Laser post-ionization and time-of-flight SIMS

The key to making the particle bombardment process more sensitive is obvious: Detect more of the particles. As mentioned above, the typical approach in SIMS and FABMS experiments is to detect the ions that are ejected from the solid. However, because in general the neutral species are much more abundant, how can we detect them? The answer to this problem lies in lasers. By irradiating a small region above the surface with a laser, it is possible to ionize the ejected species by either resonant *(4)* or nonresonant processes *(5)*.

We have chosen to use the multiphoton resonance ionization (MPRI) process because it takes less laser power to make ions than the nonresonant approach. The resonant ionization scheme for an atom such as In is shown in Figure 2. Two colors of laser light are used *(4)*. The first photon (304 nm, 0.850 mJ per pulse in this case) excites an atom from its ground electronic state to an excited state. The second photon (608 nm, 7.03 mJ per pulse) ionizes the atom from this excited state. These schemes produce ions with nearly 100% efficiency, as demonstrated so elegantly by Hurst and his co-workers during the late 1970s *(6)*. Once the neutral species have been efficiently converted to ions, the goal is to detect them with maximum efficiency.

One recent advance in mass spectrometry is the time-of-flight (TOF) reflecting mirror analyzer *(7)*. The ion to be detected is accelerated down the flight path by a high potential. The time of arrival is related to the energy and mass of the particle and the length of the flight path.

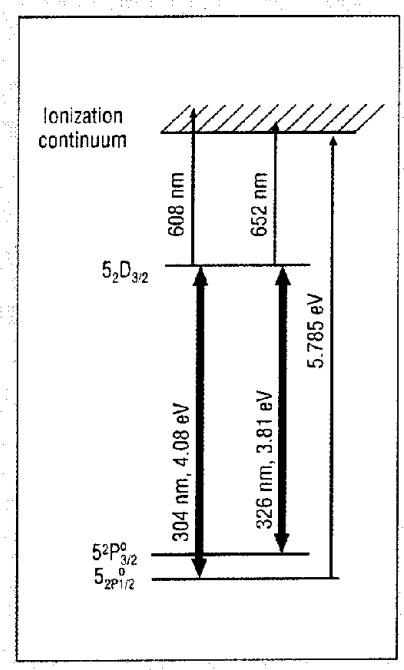

***Figure 2.* Multiphoton resonance ionization (MPRI) scheme for indium.** The first photon (304 nm or 326 nm) excites the atom while the second pulse (608 or 652) ionizes the excited state.

If all the ejected particles had the same kinetic energy at time = 0, then the energy would be the acceleration potential plus the ejection energy. The mass of the particle would be perfectly determined by the arrival time. However, there is a distribution of kinetic energies of the ejecting particles, and the time of arrival is a convoluted function of mass and the unknown kinetic energy.

To circumvent this problem the particles are decelerated at the end of the flight path, turned around, and then accelerated along a second flight path. This reflection causes a time focus at the detector and removes the kinetic energy as a parameter in the mass determination.

This type of analyzer now has a resolving power of greater than 1 part in 10,000 with an efficiency approaching 50%. It has opened the SIMS technique and its variants to be applied to the study of very high molecular weight compounds *(8)*. A schematic of a basic instrument for particle bombardment, MPRI and the TOF detection is shown in Figure 3.

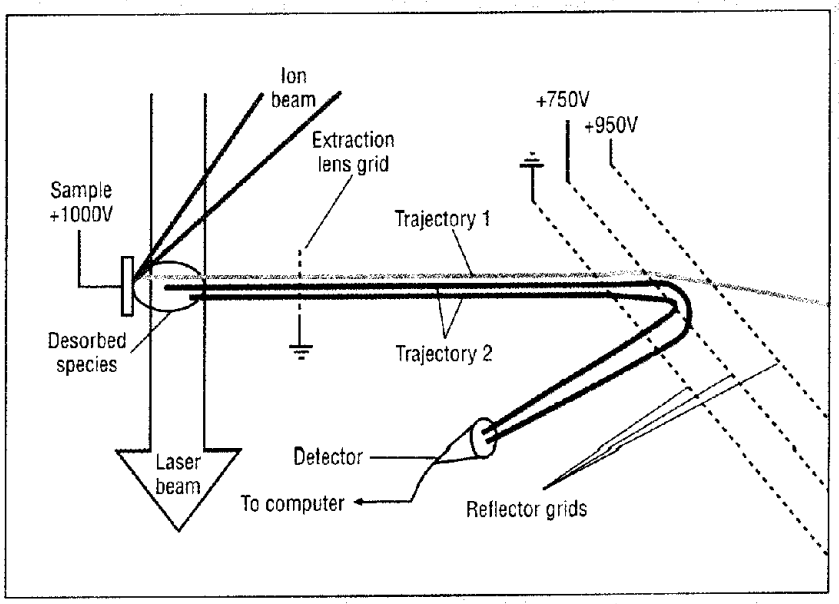

***Figure 3.* Schematic for the ion beam, MPRI, and reflecting mirror detector instrument.** Trajectory 1 is the trajectory of the ions created at the surface itself. Trajectory 2 is the trajectory of the ions created in the laser beam from the neutral species ejected from the surface.

Table 1. **MPRI experimental data for In in Si**

[In], ppb	Average signal[a]	Average background[a]	Ar^+ current, μA	Laser power, W	Relative intensity[b]
2000	1.45×10^3	18.5	0.158	0.186	$(4.84\ \text{Å} \pm 0.08) \times 10^4$
36.5	2.78×10^3	29.5	18.0	0.158	880 ± 62.4
3.85	9.41×10^2	9.6	47.3	0.211	93.7 ± 22.6
0.165	3.72×10^1	4.0	46.0	0.211	3.43 ± 0.58

[a] Signal and background are expressed as counts per 9000 laser pulses, averaged over three analyses.
[b] Relative intensity is derived by normalizing the data for each individual analysis to the ion current and laser power and obtaining a cumulative average. The results in this column have been used to generate the calibration plot. The error limits are reported at the 95% confidence level from three independent observations.

solid resulting from a single particle striking the surface, and it is amazing that any useful knowledge can be discerned about the composition or arrangement of molecules in the topmost atomic layer.

Through the use of molecular dynamics (MD) computer simulations, it is possible to gain an atomistic view of the process, which shows that many of the particles eject from the surface layer (*2*). Moreover, the particles' motions are initiated at time scales that are relatively short compared to the time scale of the damage in the solid; thus the properties of the ejected species really do reflect the arrangement of surface atoms. The picture of surface damage must be kept in mind, however, when the surface topology of an integrated circuit is being characterized or when ion beams are used to study molecular surfaces. Once a portion of the sample has been struck by an energetic particle, the surface atomic arrangement is no longer the same as it was originally. Thus for surface-sensitive applications of SIMS, the total dose of incident particles must be less than about $10^{12}/cm^2$, where typical surface densities are 10^{15} atoms/cm^2. This puts a constraint on experimental configurations.

What we're really looking at

The particles that eject from the surface are the ones that are ultimately detected in SIMS. These particles can be neutral or ionic, atoms or molecules. Moreover, they can be in ground or excited electronic, vibrational, or rotational states. The relative proportions of each depend sensitively on the electronic properties of the ejecting species and also on the original substrate (*3*). We still do not have a complete understanding of what controls, for example, the concentration of ions that eject.

Ions are the most commonly detected species and the ion concentration can vary by several orders of magnitude depending on the solid, so it has been very difficult in the past to obtain quantitative information. What we will show here is that by post-ionizing with a laser beam the neutral species that eject, the sensitivity can be enhanced by several orders of magnitude in some cases so that it becomes easier to quantify the signals. As an aside, the fact that we do not fully understand the electronic events in SIMS makes it an interesting field of study. There is physics to be learned!

The combination of laser post-ionization with SIMS that we will discuss allows us to have a surface detection limit as low as 9 atoms per trillion surface atoms. In addition, the sensitivity for detecting molecules is greatly enhanced. We will show how the liquid metal ion gun (LMIG) allows for spatial resolutions of 500–1000 Å. Finally we will discuss how these techniques are allowing us to gain a better understanding of the fundamental physics involved in keV particle bombardment.

Parts per trillion

How sensitive is this combination of laser ionization and time-of-flight mass spectrometry? We tested the combined particle beam and laser design by fabricating three samples that contained known concentrations of In in a Si wafer (*9*). In order to minimize the effects of possible contamination or surface segregation, the samples were sputtered before each data acquisition cycle until a steady-state, reproducible signal was obtained (*10*). The data were then accumulated for 5 min (9000 laser pulses at a repetition rate of 30 Hz), after which the background signal was measured for an equivalent period.

In order to detect single pulses, the photoion signal was attenuated for the two most concentrated samples by reducing the primary ion current. Individual determinations were normalized to the measured ion current and laser power. The experimental parameters and results are presented in Table 1.

Because the TOF analyzer clearly resolves both the abundant isotope ^{115}In and the less abundant isotope ^{113}In, the 3.85 ppb (part per billion) sample is also a 165 ppt (parts per trillion) sample in ^{113}In concentration. A plot of the relative MPRI intensity versus bulk In concentration is shown in Figure 4.

Although a logarithmic scale has been chosen for display purposes, the results of the least-squares analysis on the normalized linear plot denote a slope of 1.00 ± 0.01. In addition, the raw data from the analysis of the ^{113}In in Si indicate a S/N (signal/noise) ratio of about 9. If this is

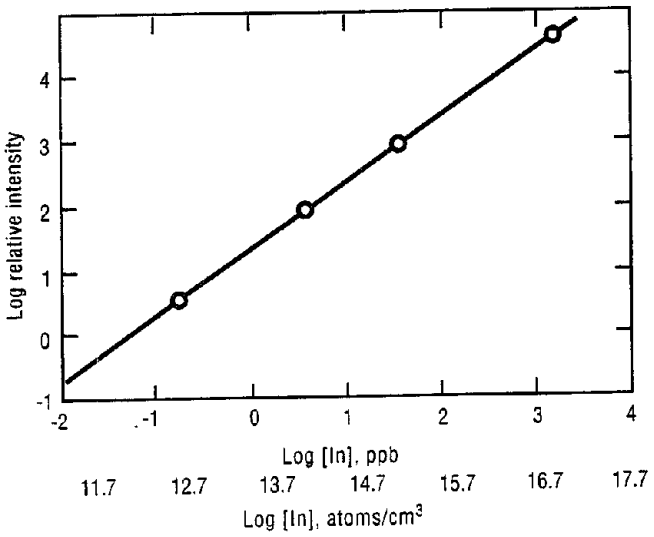

Figure 4. **The MPRI intensity of indium versus the bulk indium concentration.** The In reference concentrations (in atoms per cubic centimeter) are 1×10^{17}, 1.83×10^{15}, 1.92×10^{14}, and 8.25×10^{12}. See Table 1 for additional information.

extrapolated to S/N = 2 and a number of other corrections are applied, a detection limit of 9 ppt is obtained.

The combination of the particle bombardment and MPRI techniques allows ppt analysis of surface concentrations. Furthermore, for the 165 ppt analysis, 46 mA of primary ion current was delivered to the sample in 5.6 ms pulses. For the 5 min data accumulation period, this bombardment yielded a total dose of 1.5×10^{13} Ar ions into the 0.07 cm^2 beam spot, corresponding to a removal of 2.0×10^{13} surface atoms (0.3 monolayer) on the assumption that In desorbs at the same rate (1.4 atoms per incident ion) that has been observed for Si (*11*). Given the detection limit of 9 ppt, this experiment is therefore sensitive to 180 atoms. If removal of an entire monolayer is required, then as few as 640 atoms may be detected.

Now that the applicability of the combined technique has been shown for atoms, can it do the same wonders for molecules?

Detection of surface molecules

The techniques of SIMS and FABMS have opened the door to high molecular weight mass spectrometry (*12*), but the energy level diagram for molecules is not as simple as that shown in Figure 2 for In atoms. In addition to the electronic levels there are a multitude of vibrational and rotational levels. Furthermore, when a molecule is ejected from the surface it is invariably in one of these excited vibrational or rotational states. Thus, finding a perfect resonance is both easy and hard. If there is an easily accessible electronic state, then finding a density of molecules in a given vibration/rotation level where they can be ionized is easy. Unfortunately, sometimes species show up that one does not expect. In addition, the photon field may also dissociate the molecule, leading to fragmentation. The area of the control of laser-induced photofragmentation is obviously one that is ripe for exploration.

As a model system to study this problem, we have chosen a set of polycyclic aromatic compounds (PACs) for evaluating the characteristics of this approach. The compounds are environmental health hazards because of their acute carcinogenic and mutagenic behavior. Moreover, there are many applications where surface detection of PACs is desirable without resorting to elaborate sample pretreatment. Our results show that, indeed, it is possible to characterize small fractions of a monolayer of PACs on both conducting and insulating surfaces with subfemtomole detection limits (*13*).

Benzo[a]pyrene ($C_{20}H_8$, mass = 252 amu) is one of the most toxic and carcinogenic PACs. The detection of this particular molecule, which is present in trace amounts in soil, air, and water samples, is of widespread interest. The experiments we performed were done in basically the same manner as the In experiments described above. In this case both photons have energies of 280 nm, as two of these photons have sufficient energy to ionize most PACs. Figure 5a shows the SIMS spectrum with the parent peak barely discernible. Figures 5b-e show the MPRI-TOF spectra obtained as a function of laser intensity. Even at the lowest laser intensity the parent peak is dominant. The spectrum at 3.0×10^5 W/cm^2 (5d) is about 1000 times more intense than in the SIMS spectrum. The detection limit for this case is about 10^6 molecules/cm^2. As the laser power is increased (5e) the parent peak remains but the fragmentation pattern changes. This kind of "tunable" fragmentation has been observed before and can be employed as a means of sequencing proteins (*14*).

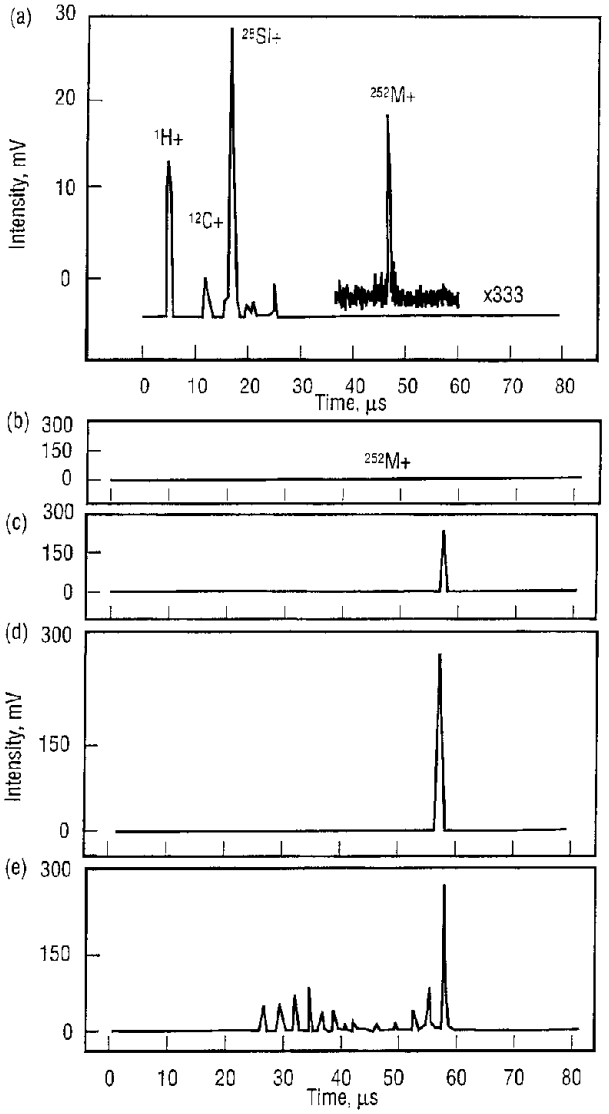

Figure 5. **Time-of-flight spectra of benzo[a]pyrene ions desorbed from a silicon surface.** (a) Positive secondary ion mass spectometry (SIMS) spectrum using a 815-ns incident Ar^+ ion pulse. (b–e) MPRI mass spectra at various 280-nm laser intensities in W/cm^2: (b) 1.9×10^4; (c) 1.2×10^5; (d) 3.0×10^5; (e) 2.0×10^6.

Control over molecular ion fragmentation opens the possibility for the direct analysis of mixtures of closely related PACs using MPRI detection. To demonstrate this possibility, we prepared a simulated sample consisting of benzo[a]pyrene, dibenz[ac]anthracene, triphenylene, and pyrene (*13*). A 1:1 benzene solution with all four molecules was deposited onto a clean wafer and air dried. The theoretical concentration of each molecule in the analysis zone was about 10^{-12} mole assuming uniform deposition.

The MPRI-TOF spectrum of the mixture for a modest laser power density of approximately 1×10^6 W/cm^2 at 280 nm photon wavelength is shown in Figure 6. There are three intense peaks associated with benzo[a]pyrene, dibenz[ac]anthracene and triphenylene, and a lower intensity pyrene signal. Note that the peak intensities for all four molecules are not equal, even though the solution was equimolar with respect to each compound. There are several possible explanations for the observed intensity variations: nonuniform distribution of samples across the target, different photoabsorption cross sections leading to nonuniform detection efficiencies, and different sublimation rates

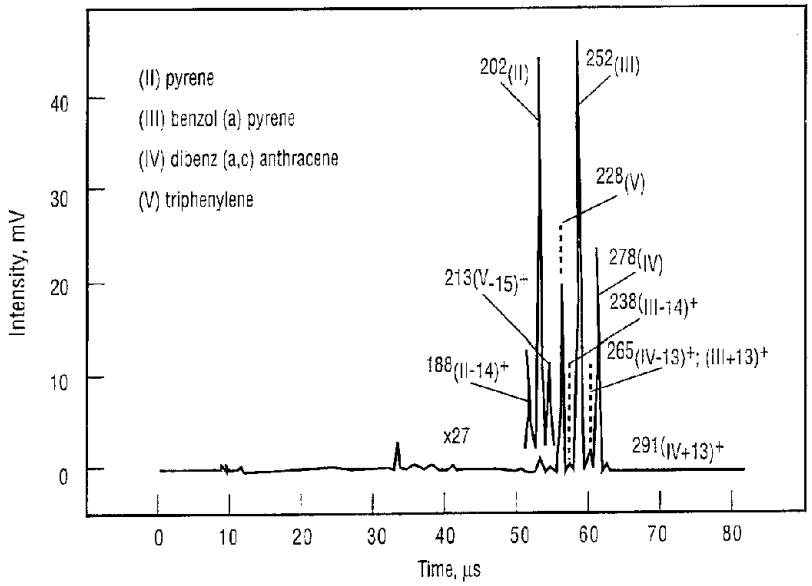

***Figure 6.* Time-of-flight MPRI mass spectrum of a simulated complex mixture.** The spectrum was obtained by use of 10^{-12} mol of each PAC labeled in the insert. MPRI was accomplished with a 280-nm laser radiation at a power density of 1.6×10^6 W/cm^2.

due to different vapor pressures of each compound. Nonetheless, these preliminary results suggest that direct mixture analysis will be an important future application of this methodology.

Opening the door for spatial resolution

The combination of keV particle beams, laser post-ionization and time-of-flight mass determination has made it possible to perform surface-sensitive trace analysis. The next big breakthrough comes from the use of the liquid metal ion gun (LMIG), which allows for 500–1000 Å spatial resolution.

The LMIG used as a SIMS source is constructed from a sharp tungsten or other hard metal tip. A liquid metal such as Ga or In is allowed to "drain down" the tip, at which time a large extraction voltage is applied. The result is that the Ga or In ions stream off the small tip at energies of the order 25–60 keV in a highly focused beam. It is this focused quality of the LMIG that allows for spatial imaging with SIMS.

Using a LMIG with a conventional SIMS detection scheme (quadrupole) Levi-Setti and co-workers, who pioneered this work in the early 1980s (*15*), have examined several silver halide-based emulsion microcrystals engineered for photographic applications. The complex compositional structure and small size (<2 μm) of these fragile species imposes stringent requirements on any technique employed to measure them. Figure 7 is a SIMS map using an LMIG to examine photographic silver iodobromide crystals. Analysis of the $^{79}Br^+$ SIMS image on the left of Figure 7 indicates that the triangular or hexagonal crystals are uniform in bromine construction. The I^- SIMS image on the right shows that the iodine is concentrated on the edges of the crystals and is low in concentration in the center. These observations do not agree with those predicted by precipitation chemistry (*16*).

The future

We can now meld together ion beam methods, TOF mass detection, liquid metal ion guns, and multiphoton resonance ionization to produce real maps of the surface distribution of atoms and molecules. We have used this combined technique to obtain spatially resolved maps of the In signal (*21*). A 300-mesh Cu grid was placed over an In foil so as to shadow specific regions of the In surface (Figure 8). For this particular image, each pixel measures 5000 Å × 5000 Å and the total field of view is 150 × 150. Each pixel was produced by summing the results of two laser shots. The image, which contains 50,000 pixels, was recorded in 45 min. We estimate that the data acquisition efficiency can be improved by a factor of 4 when using a transient digitizer rather than a multihit time to digital converter. Moreover, if the LMIG is employed using the larger aperture, the count rates improve by an additional factor of 8 with only a small loss in spatial resolution.

Will it be possible to record comparable images for molecules on a surface? Based on the In map shown in Figure 10 along with the MPRI spectra of molecules such as those in Figure 5, we obviously believe that this is the future. Michael Kelley was indeed right in 1987. Ion beams are attracting more attention. Moreover, the coupling with lasers has considerably brightened their future.

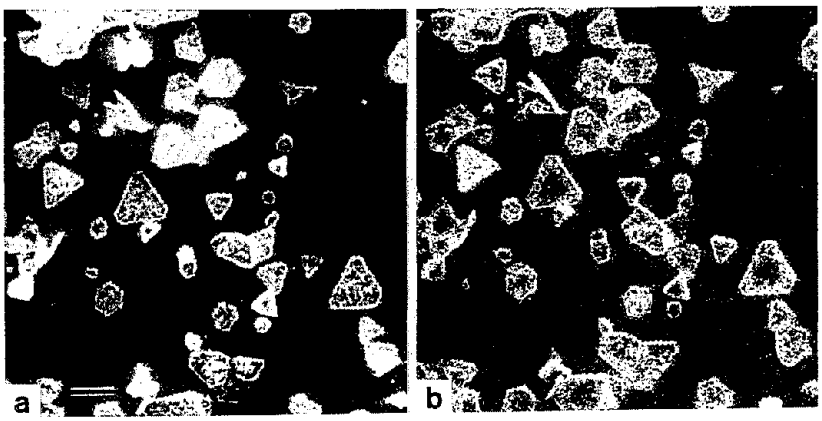

***Figure 7.* SIMS maps of engineered photoemulsion microcrystals containing a pure AgBr core and concentric shells containing 8 wt% I and 16 wt% I.** Scale bar = 2 μm. (a) This Br^- image shows triangular or hexagonal crystals uniform in bromine concentration. (b) The I^- image shows iodine concentrated on the edges of the crystals and is very low in concentration in the center.

Acknowledgment

We gratefully acknowledge the support of the National Science Foundation, the Department of Energy, and the Office of Naval Research.

It is possible to use the timing between the keV ion pulse and the laser pulse for a different time-of-flight measurement: that of the velocity of the ejected atoms. This allows us to determine atomic level properties and permits us to understand crystal behavior under keV bombardment.

In the experimental configuration and timing sequence shown in Figure 3, the TOF was used after the laser pulse to do the mass determination. However, this is a bit redundant as the resonant ionization process already selectively picks the mass, especially if we restrict ourselves to atoms. Thus by changing the time delay between the ion pulse and the laser pulse, the velocity or energy distribution can be measured. If a flat plate detector replaces the TOF analyzer, it is also possible to determine the takeoff angle of the desorbing species, and both the energy and angle distributions can be simultaneously measured *(17)*. These distributions are most interesting for single crystals as there are strong angular effects.

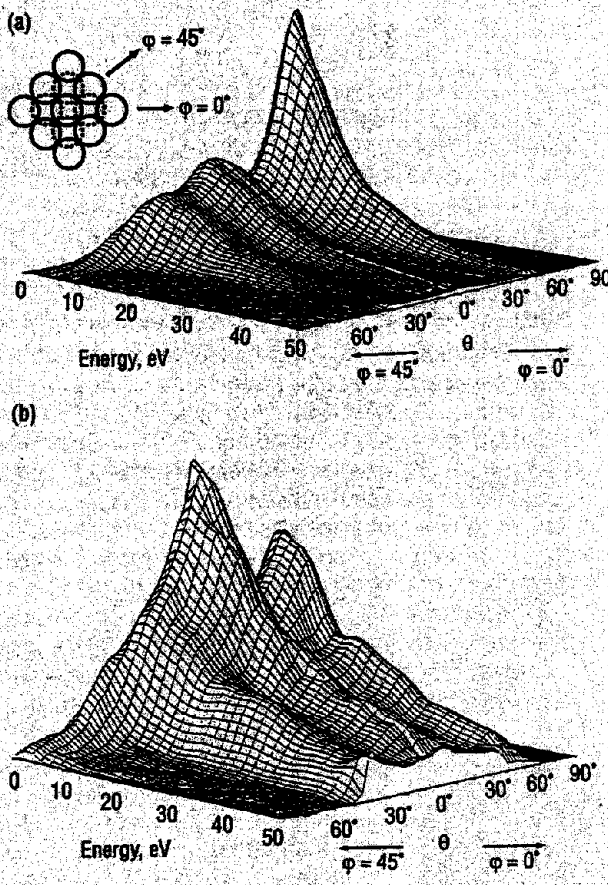

Figure 9. **Energy- and angle-resolved distributions of Rh atoms ejected from 5 keV Ar^+ ion bombardment Rh (100).** (a) $^4F_{9/2}$ orbital ground state; (b) $^4F_{7/2}$ excited state. The data correspond to ejection along $\phi = 0°$ and $\phi = 45°$ crystallographic directions, as defined in the inset. Owing to the symmetry of the surface and the angular resolution (e.g., $\Delta\phi = 18$ at $\theta = 45$), the results represent the data over about 50% of all space. Both plots are normalized to the maximum intensity peaks. The dashed circles in the inset represent second layer atoms.

The energy and angle distributions for the ground $^4F_{9/2}$ state of Rh are shown in Figure 9a. The energies of the ejected atoms range from 0 to >50 eV. The polar angle, θ, is 0° for emission perpendicular to the surface and 90° for grazing angles. Without belaboring the details, the distribution has characteristic features with the largest peak in the $\phi = 0°$ direction *(18)*. By slightly changing the wavelength of the laser to something like that depicted in Figure 2 for In, the $^4F_{7/2}$ excited state of Rh can be accessed. Figure 9b is the distribution for the excited state of Rh. It is different from the ground state. These distributions represent the first obtained for two separate states where the intensities have been measured at all angles for energies between 0 and 50 eV. Previous work was limited to one angle of ejection.

Detailed data such as these challenge theories and theorists to the limit. The traditional model of the velocity distribution of excitation predicts that the ratio of the excited state intensity to the ground state intensity should go as $\exp(-A/av_\perp)$, where A and a are constants and $v_\perp$ is the perpendicular component of the ejection velocity *(19)*. A plot of the log of this ratio versus $1/v_\perp$ (Figure 10) shows that at high velocities the data follow the simple model. However, at low velocities, there is no velocity dependence. A model for the excitation and de-excitation process has been incorporated into the molecular dynamics calculations and the results from these calculations are also shown in Figure 10. The agreement is very good. Moreover, the calculations tell us that collisions of ejecting particles within 1–20 Å over the surface gives rise to the plateau seen in the experimental distribution *(20)*.

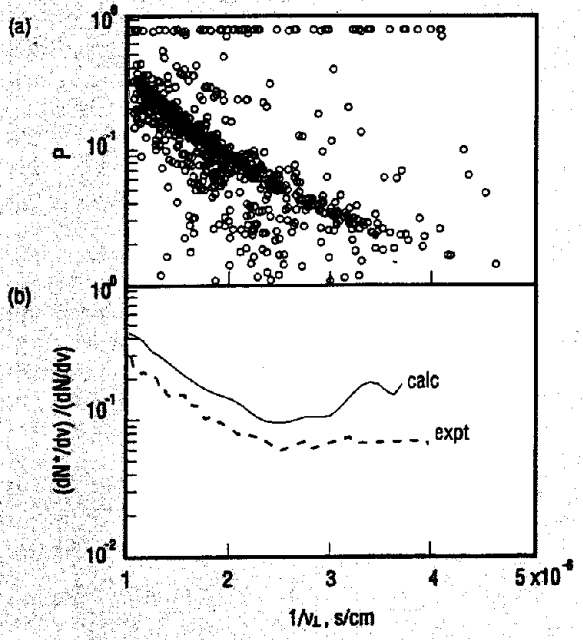

Figure 10. **Excitation probabilities.** (a) Calculated excitation probabilities, P, of individual atoms vs $1/v_\perp$ for $\theta < 30°$. (b) Ratio of intensities $(dN^*/dv)/(dN/dv)$ as obtained from the averaged excitation probability. The solid line includes all sputtered atoms in the calculation. The dashed line represents the experimental data.

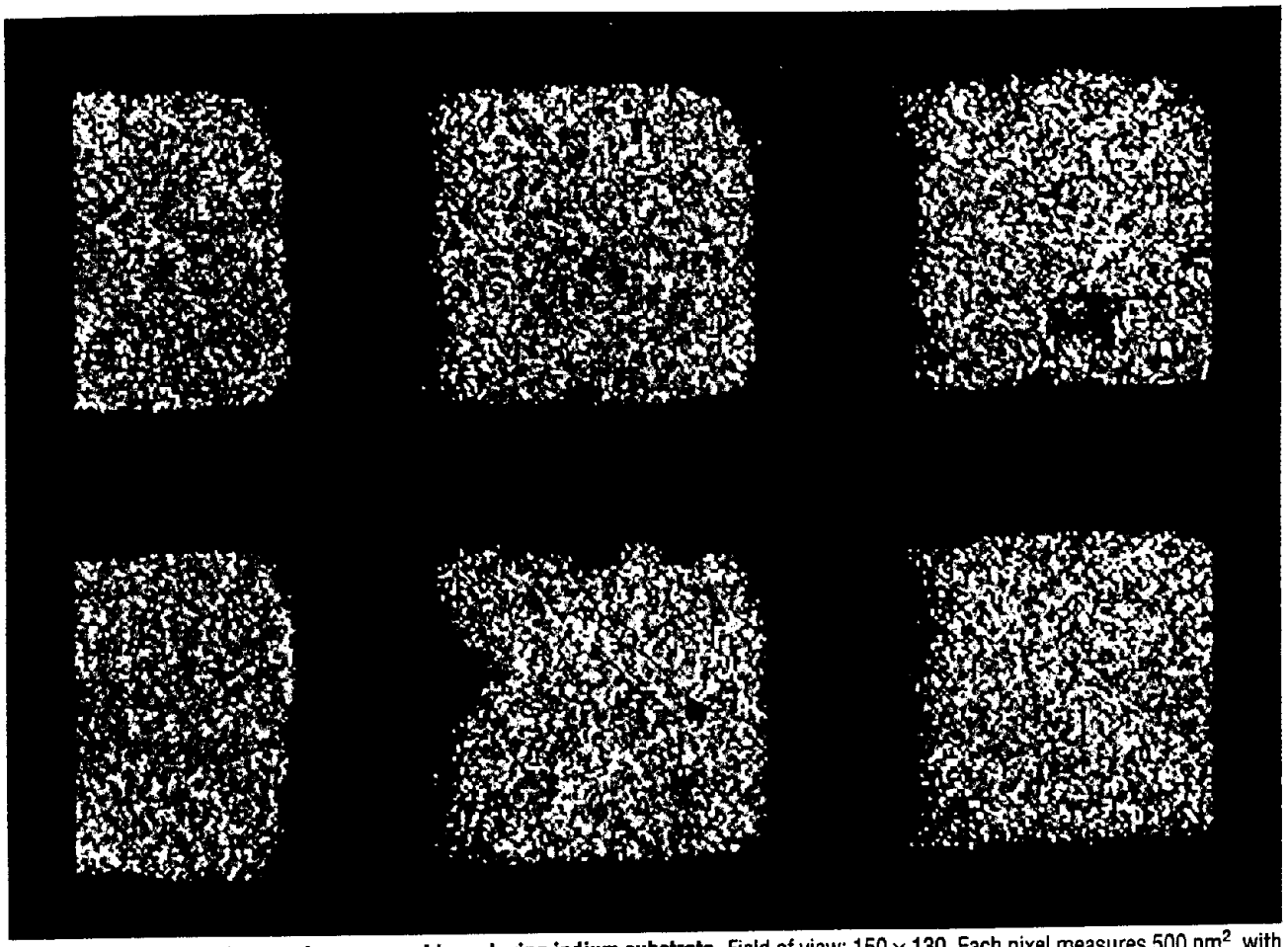

Figure 8. **Indium atom image of a copper grid overlaying indium substrate.** Field of view: 150 × 130. Each pixel measures 500 nm^2, with the brightest pixels containing 18 counts. 1×10^5 pulses, total dose 2×10^7 Ga^+ ions or 10^{11} Ga^+ ions/cm^2.

References

(1) Kelley, M. J. CHEMTECH, May 1987, p. 294.
(2) Harrison, D. E., Jr.; Kelly, P. W.; Garrison, B. J.; Winograd, N. *Surf. Sci.* **1978**, *76*, 311.
(3) Winograd, N.; Garrison, B. In *Methods of Surface Characterization*; Czandema, A. W.; Hercules, D. M., Eds.; Plenum: New York, 1991; vol. 2, p. 45.
(4) Winograd, N.; Baxter, J. P.; Kimock, F. M. *Chem. Phys. Lett.* **1982**, *88*, 581.
(5) Becker, C. H.; Gillen, K. T. *Appl. Phys. Lett.* **1984**, *45*, 1063.
(6) Hurst, G. S.; Payne, M. G.; Kramer, S. D.; Young, J. P. *Rev. Mod. Phys.* **1979**, *51*, 767.
(7) Mamyrin, B. A.; Karataev, V. I.; Shmikk, D. V.; Zagulin, V. A. *Soviet Physics-JETP* (Engl. Trans.) **1973**, *37*, 45.
(8) Chait, B. T.; Standing, K. G. *Int. J. Mass Spectrom. Ion Phys.* **1981**, *40*, 185.
(9) The Si targets were supplied by M. Young of Hughes Research Laboratories and J. E. Parks of Atom Sciences, Inc. The wafers were prepared by liquid-encapsulated Czochralski (LEC) single-crystal growth, and the In concentrations were determined by bulk resistivity measures. All other dopants (excluding oxygen) were present at less than 10^{13} atoms per cubic centimeter.
(10) Pappas, D. L.; Hrubowchak, D. M.; Ervin, M. H.; Winograd, N. *Science* **1989**, *243*, 64.
(11) Wittmaack, K. In *Inelastic Ion-Surface Collisions*; Tolk, N. H; Tully, J. C.; Heiland, W.; White, C. W., Eds. Academic: London, 1977; p. 153.
(12) *Secondary Ion Mass Spectrometry, SIMS VII*; eds. Benninghoven, A.; Evans, C. A.; Mickeegan, K. D.; Storms, H. A.; Werner, H. W., Eds.; John Wiley and Sons: New York, 1990.
(13) Hrubowchak, D. M.; Ervin, M. H.; Winograd, N. *Anal. Chem.* **1991**, *63*, 225.
(14) Grotemeyer, J.; Schlag, E. W. *Org. Mass Spect.* **1988**, *23*, 288.
(15) Levi-Setti, R.; Hallegot, P.; Girod, C.; Chabala, J. M.; Li, J.; Sodonis, A.; Wolbach, W. *Surf. Sci.* **1991**, *246*, 94, and references therein.
(16) Chabala, J. M.; Levi-Setti, R.; Harvey, K. N.; Maternaghan, T. J.; Tyler, A.; Loretto, M. H.; Berry, F. J. In *SPSE 43rd Ann. Conf., Rochester, NY*; SPSE: Springfield, Va., 1990; p. 40.
(17) Winograd, N.; Kobrin, P. H.; Schick, G. A.; Singh, J.; Baxter, J. P.; Garrison, B. J. *Surf. Sci. Lett.* **1986**, *176*, L817.
(18) Winograd, N.; El-Maazawi, M.; Maboudian, R.; Postawa, Z.; Bernardo, D. N.; Garrison, B. J. *J. Chem. Phys.* **1992**, *96*, 6314.
(19) Hagstrum, H. D. *Phys. Rev.* **1954**, *96*, 336.
(20) Bernardo, D. N.; Garrison, B. J.; El-Maazawi, M.; Maboudian, R.; Postawa, Z.; Winograd, N. *J. Chem. Phys.* **1992**, *97*, 3846.
(21) Winograd, N.; Zhou, Y.; Wood, M.; Lakiszak, S.; Mullock, S. *Proc. Resonance Ionization Spectrosc.*, in press.

Barbara J. Garrison is a Professor and Head of the Chemistry Department at Penn State University, where she researches the computer modeling of gas–surface reactions such as keV particle bombardment, molecular beam epitaxial growth of semiconductors, fluorine etching of silicon, and diamond film growth. She is a member of the NSF Chemistry Advisory Committee and the Editorial Board of *Accounts of Chemical Research*. Her education includes a B.S. in Physics from Arizona State and a Ph.D. in Chemistry from UC, Berkeley.

Nicholas Winograd is an Evan Pugh Professor of Chemistry at Penn State University (152 Davey Laboratory, University Park, PA 16802; 814-863-0001). His research is aimed toward utilizing the fundamental aspects of ion/solid interactions in surface chemistry studies. He has received numerous prizes and awards and is the co-author of more than 185 publications. His education includes a B.S. in Chemistry from Rensselaer and a Ph.D. from Case Western Reserve.